ARTICLE

Conformations and Structures of Ethoxycarbonyl Isothiocyanate Revealed by Rotational Spectroscopy

Yugao Xu, Wenqin Li, Jiaqi Zhang, Gang Feng*

School of Chemistry and Chemical Engineering, Chongqing University, Chongqing 401331, China

(Dated: Received on September 26, 2021; Accepted on October 17, 2021)

The ethoxycarbonyl isothiocyanate has been investigated by using supersonic jet Fourier transform microwave spectroscopy. Two sets of rotational spectra belonging to conformers TCC (with the backbone of C−C−O−C, C−O−C=O, and O−C(=O)−NCS being *trans*, *cis*, and *cis* arranged, respectively) and GCC (*gauche*, *cis*, and *cis* arrangement of the C−C−O−C, C−O−C=O, and O−C(=O)−NCS) have been measured and assigned. The measurements of ^{13}C, ^{15}N and ^{34}S mono-substituted species of the two conformers have also been performed. The comprehensive rotational spectroscopic investigations provide accurate values of rotational constants and ^{14}N quadrupole coupling constants, which lead to structural determinations of the two conformers of ethoxycarbonyl isothiocyanate. For conformer TCC, the values of P_{cc} keep constant upon isotopic substitution, indicating that the heavy atoms of TCC are effectively located in the *ab* plane.

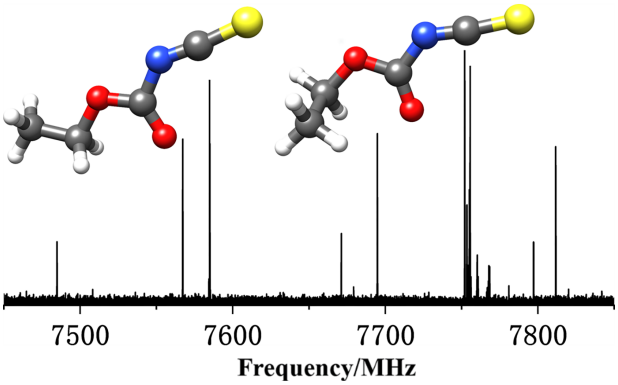

Key words: Microwave spectroscopy, Interstellar molecule, *Ab initio* calculation, Structural analysis, Supersonic expansion

I. INTRODUCTION

Isothiocyanates (R-NCS) are important reagents for synthesis of heterocyclics, pesticides and drugs, which therefore have widely pharmaceutical and industrial applications [1−3]. Isothiocyanates themselves show a variety of biological activities and can be used as cancer treatment, antioxidant, anti-inflammatory, and antibacterial drugs [4, 5]. For example, allyl isothiocyanate, a natural compound found in cruciferous plants, can inhibit microbial growth [6, 7], and also shows strong antibacterial activity [8−14]. The reactivity and bioactivity of these compounds are unquestionably determined by their conformations and structures. Spectroscopic characterizations of this kind of compounds have been carried out for those alkyl isothiocyanates [15−17], alkenyl or alkynyl isothiocyanates [18−20], carbonyl isothiocyanates [21−25], alkoxy isothiocyanates [26], as well as phenyl isothiocyanate [27], providing detailed information on the conformational landscape and the structures. Among the commonly used experimental techniques, Fourier transform microwave (FTMW) spectroscopy coupled with supersonic expansion [28−31] can precisely determine the structure of targeted molecules undisturbed by crystal or solvent effect.

In addition, isothiocyanates are potential molecular species that may be prevalent in interstellar and circum-

*Author to whom correspondence should be addressed. E-mail: fengg@cqu.edu.cn

stellar media. Indeed, HNCS [32] and its isomeric structure of HSCN [33], as well as thiocyanogen (NCS) [34] have been identified in the chemically rich interstellar regions. These observations suggest that structural complex molecules containing isothiocyanate group may exist in space, also considering that many complex organic molecules have been detected [35]. This calls for accurate laboratory rotational spectroscopic measurements of these potential interstellar molecules which serve as important references for identifying molecules in the observed data set.

Rotational spectroscopic investigations have been reported for isopropyl isothiocyanate [17, 36], ethynyl isothiocyanate [19], allyl isothiocyanate [37], vinyl isothiocyanate [20, 38], cyanogen isothiocyanate [39, 40], phenyl isothiocyanate [41], and methyl isothiocyanate [42]. These studies provide detailed structural information and accurate rotational transition frequencies. In this work, we probe the conformations and determine the molecular structure of an isothiocyanate containing an ester substituent, *i.e.*, ethoxycarbonyl isothiocyanate ($CH_3CH_2OC(=O)NCS$, EIC in short), using pulsed supersonic-jet FTMW spectroscopy. *Ab initio* calculations are implemented to support the spectral analysis and supply additional energetic and structural information on the conformational preferences.

II. EXPERIMENTAL AND THEORETICAL METHODOLOGIES

Commercial sample of EIC (Adamas, ∼98% in purity) was directly used for the measurements. The rotational spectra of EIC in range of 2−20 GHz were obtained using a homebuilt pulsed supersonic-jet FTMW spectrometer [28] as detailed elsewhere [29, 43]. The sample of EIC (∼1 mL) was reserved in a stainless reservoir and placed in the upstream of the pulse valve. The temperature of reservoir was maintained at 323 K to increase the vapor pressure of EIC. Helium was taken as the carrier gas and maintained at 2 bars, which was allowed to flow over EIC and was expanded into the resonator of the spectrometer through a Parker General solenoid valve (0.5 mm diameter orifice). The molecules in the supersonic jet were polarized by pulsed microwave radiation which induced free induction decay. The time-domain signals were measured and Fourier-transformed to generate the frequency domain spectrum. Spectral survey was achieved by a step-by-step scan (0.4 MHz step with 512 averaged cycles for each step). Measurements for weak signal were implemented by increasing the accumulation cycles up to tens of thousands. Each rotational transition appeared as two components due to the co-linearity configuration of the supersonic-jet and the microwave propagation.

Quantum-chemical computations were carried out using the Gaussian 16 program [44]. All the possible conformations of EIC were geometrically optimized at the MP2/6-311++G(d,p) [45, 46] level of theory. Harmonic frequency calculations at the same level were performed to verify that the obtained structures are real minima.

III. RESULTS AND DISCUSSION

A. *Ab initio* calculations

The orientations of the C1−C2−O3−C4, C2−O3−C4−O8 and O8−C4−N5=C6 skeletons (See FIG. 1 for the atom numbering) of EIC determine its conformational potential energy surface (PES). The orientation of C1 can be *gauche* (G) or *trans* (T) to C4 which corresponds to a value of 0° or ±60° of the ∠(C1C2O3C4) dihedral angle, respectively. The C2−O3−C4−O8 and O8−C4−N5=C6 skeletons can be either *cis* (C), or T oriented, respectively. In total, there are 8 possible configurations for EIC monomer (FIG. S1 in Supplementary materials (SM)). Seven local minima of EIC are obtained from *ab initio* calculations (FIG. 1), which are named according to the three dihedral angles of ∠(C1C2O3C4), ∠(C2O3C4O8) and ∠(O8C4N5C6) with C, G, or T indicating values of 0°, ±60°, or 180°, respectively.

The most stable conformation of EIC (TCC) has *trans*, *cis*, and *cis* orientation of the C1−C2−O3−C4, C2−O3−C4−O8 and O8−C4−N5=C6 units, respectively. Conformer GCC is 102 cm^{-1} higher in energy than TCC. Conformer TCT is 163 cm^{-1} higher in energy than TCC with the O8−C4−N5=C6 skeleton being *cis* arrangement. Conformer GCT has C1−C2−O3−C4 skeleton *gauche* arrangement and O8−C4−N5=C6 skeleton *trans* arranged, which has a relative energy of 237 cm^{-1}. The values of relative energy of conformers TTC, GTC and TTT are calculated to be greater than 1200 cm^{-1}. The calculated rotational constants, ^{14}N nuclear quadrupole coupling constants, and the electric dipole moment components of the 7 conformers are presented in Table S1 (Supplementary materials). The spectroscopic parameters of conformers TCC and GCC are also given in Table I and Table

DOI:10.1063/1674-0068/cjcp2109177

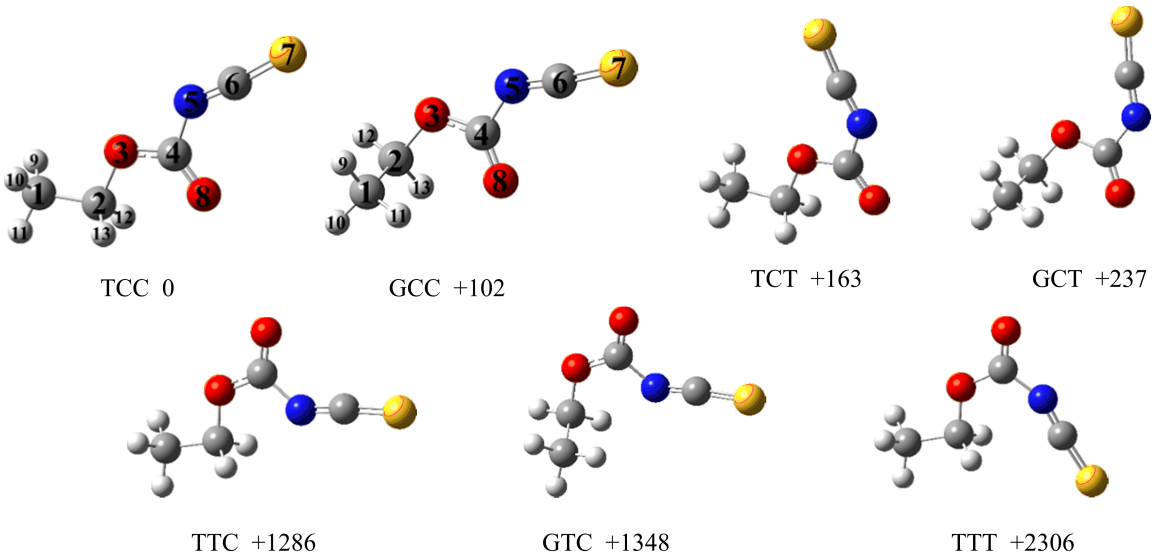

FIG. 1 Geometries and relative energies (zero-point corrected, given in cm^{-1}) of the seven minima conformations of EIC obtained at the MP2/6-311++G(d,p) level of theory. The atomic numbering of the first two conformers is also indicated.

TABLE I The determined spectroscopic parameters of the most abundance species (parent) and six mono-substituted isotopologues of conformer TCC. Equilibrium rotational constants calculated at the MP2/6-311++G(d,p) level of theory are also included for comparison.

Species	A/MHz	B/MHz	C/MHz	σ^a/kHz	N^b	P_{cc}/uÅ^2
TCC(MP2)	7952.1940 (−0.1%)[c]	617.8712 (−0.5%)	577.4846 (−0.5%)	/	/	3.175
Parent[d]	7963.4357(4)[e]	621.03240(5)	580.51611(4)	2.9	240	3.33318(9)
^{13}C1	7899.6(2)	609.43233(6)	570.04179(6)	2.2	74	3.336(2)
^{13}C2	7952.9(3)	615.00037(7)	575.18697(7)	2.7	71	3.333(2)
^{34}C4	7950.3(3)	620.86668(6)	580.30212(6)	2.3	75	3.334(2)
^{13}C6	7953.4(4)	618.52634(8)	578.27312(7)	2.8	69	3.333(3)
^{15}N5	7951.7(8)	620.8666(2)	580.3018(2)	6.1	23	3.328(6)
^{34}S7	7957.5690(7)	604.40864(5)	565.93551(5)	3.2	116	3.3331(1)

[a] Root-mean-square deviation of the fit.
[b] Number of transitions included in the fit.
[c] The percentage in parentheses is the deviation between theoretical rotational constants and those of experimental ones.
[d] The D_J, D_{JK}, $1.5\chi_{aa}$, and $0.25(\chi_{bb}-\chi_{cc})$ have been determined to be 0.0130(2) kHz, 1.279(4) kHz, 2.754(5) MHz, and −0.1324(9) MHz for the parent species, respectively. These parameters have been kept fixed in spectral fits of the mono-substituted isotopologues.
[e] Values in the parentheses are 1σ errors given in units of the last digit.

II, and compared with the experimental values, respectively.

B. Rotational spectra

Guided by the *ab initio* results (FIG. 1 and Table S1 in SM), rotational spectral survey for conformer TCC was carried out firstly. Groups of rotational transitions showing *a*-type *R*-branch band features are identified and assigned to this conformer. All the observed transitions show hyperfine structures due to the ^{14}N quadruple coupling effect. FIG. 2(a) shows the ^{14}N quadruple coupling splitting hyperfine structure of the $(J+1)_{KaKc}\leftarrow J_{KaKc}=8_{08}\leftarrow 7_{07}$ transition of conformer TCC. Later on, other *a*-type and *b*-type transitions belonging to TCC were measured. No *c*-type transitions could be measured due to the zero dipole component along *c*-axis.

Then some of the unidentified lines in the spectra can be assigned to conformer GCC. For this conformer, 154 *a*-type transitions and 22 *b*-type transitions are measured. None of the *c*-type transitions could be observed

DOI:10.1063/1674-0068/cjcp2109177

TABLE II The experimentally determined spectroscopic parameters of the parent and ^{34}S mono-substituted isotopologues of conformer GCC. Equilibrium rotational constants calculated at the MP2/6-311++G(d,p) level of theory are also included for comparison.

Species	A/MHz	B/MHz	C/MHz	σ^{a}/kHz	N^{b}	P_{cc}/uÅ^2
GCC(MP2)	7031.5428 (−1.4%)[c]	656.3104 (0.1%)	636.1124 (−0.1%)			23.711
Parent[d]	7130.3494(7)[e]	655.88429(8)	636.39325(6)	3.6	186	23.6389(1)
^{34}S7	7128.0(5)	638.05876(7)	619.62389(7)	2.5	68	23.668(5)

[a] Root-mean-square deviation of the fit.
[b] Number of transitions included in the fit.
[c] The percentage in parentheses is the deviation between theoretical rotational constants and those of experimental ones .
[d] The D_J, D_{JK}, $1.5\chi_{aa}$, and $0.25(\chi_{bb}-\chi_{cc})$ have been determined to be 0.0575(3) kHz, −1.837(6) kHz, 3.07(2) MHz, and −0.203(2) MHz, respectively, for the parent species. These values has been fixed in the fit of the ^{34}S isotopologues.
[e] Values in the parentheses are 1σ errors given in units of the last digit.

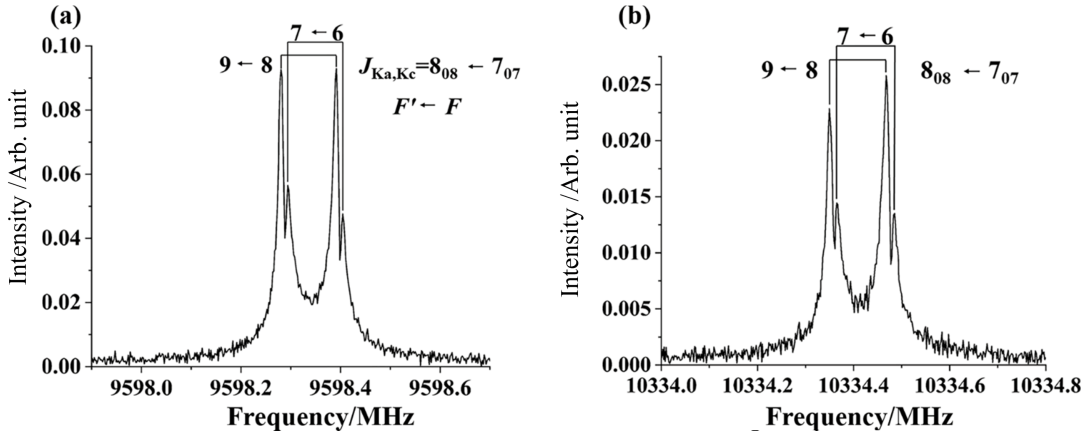

FIG. 2 The $8_{08}\leftarrow 7_{07}$ transition of (a) TCC and (b) GCC showing the ^{14}N nuclear quadrupole coupling splitting. Doppler effect induces further double splitting for each line.

in consistence with the small value of c-dipole moment component (0.2 Debye). The ^{14}N quadruple coupling hyperfine structure for conformer GCC are also resolved as shown in FIG. 2(b) for the $8_{08}\leftarrow 7_{07}$ transition. These two sets of rotational spectra are fitted independently according to a semi-rigid Hamiltonian (S-reduction and I^r representation) [47] using the SPFIT/SPCAT program [48]. The obtained values of spectroscopic parameters are reported in Tables I and II for conformers TCC and GCC, respectively.

The rotational spectroscopic investigations are extended to all the ^{34}S, ^{13}C, and ^{15}N mono-substituted isotopologues for TCC in natural abundance. However, for GCC, the signals are weak so that only the mono-substituted ^{34}S isotopologue could be measured. For all these isotopologues, the measured transition frequencies are analyzed similar to the fitting procedure of the parent species. The results obtained for all the isotopologues of conformer TCC and GCC are collected in Table I and Table II, respectively. All the fitted transition lines are given in Tables S2−S10 in Supplementary materials. Subsequently, we performed spectral surveys for conformers TCT and GCT. However, no transition lines can be assigned to these two conformers. Conformers TCT and GCT are 163 cm^{-1} and 237 cm^{-1} higher in energy than conformer TCC. The PESs connecting the conformational interconversion from high energy conformers to low ones were calculated (FIG. S3 in SM). The barriers determining the relaxation of GCC to TCC, TCT to TCC, and GCT to GCC are calculated to be 325 cm^{-1}, 415 cm^{-1}, and 446 cm^{-1}, respectively. These barrier heights indicate that conformational relaxation can take place in the supersonic jet [49]. However, considering the experimental fact that conformer GCC has been detected in the jet, the non-detection of conformers TCT and GCT is mostly due to their small amount of population in the jet expansion which leads to weak undetectable spectral signals. Other conform-

DOI:10.1063/1674-0068/cjcp2109177

ers (TTC, GTC and TTT) lie in much high energy (>15 kJ/mol) and therefore are hardly populated in the jet.

C. Discussion

Conformer TCT is calculated to be 163 cm^{-1} less stable than TCC while GCT is 135 cm^{-1} less stable than GCC, indicating that the *cis* arrangement of the NCS group to the C=O is energetically preferred. The *trans* arrangement of the C2−O3−C4−O8 backbone results in much higher energy conformations (>1200 cm^{-1}). In order to understand the possible intramolecular interactions that determine the conformational preferences, we performed molecular electrostatic surface potentials (MESPs) calculations for conformers of TCC, GCC, TCT and GCT. As reported in FIG. 3, the MESPs of the four conformers possess multiple positive and negative potential regions, with the O8 lone-pair electrons presenting the most negative electrostatic potential region (−33.0 kcal/mol to −37.7 kcal/mol) and the surface of carbonyl carbon (C4) corresponding to the most positive electrostatic potential region (24.0 kcal/mol to 26.5 kcal/mol). For TCC and GCC, the most negative values of the electrostatic potential of O3 and N5 is about −23 kcal/mol and −20 kcal/mol, respectively, significantly higher than those of O8 and N5 of conformers TCT and GCT (−37 kcal/mol and −25 kcal/mol, respectively), suggesting the electronic density difference associated with the conformational preferences. The calculated MESPs also indicate the positive and negative sites that can be involved in forming non-covalent interactions of these conformers.

We observe two sets of rotational spectra of EIC in the helium supersonic jet. The spectral carriers are confirmed to be conformers of TCC and GCC by comparing the experimental values of rotational constants, planar moment of inertia P_{cc} and ^{14}N quadruple coupling constants to those calculated ones (Tables I and II). The structural assignments are further verified by measuring and analyzing the $^{13}C1$, $^{13}C2$, $^{13}C4$, $^{15}N5$ and $^{34}S7$ isotopic spectra of TCC (Table I) and the $^{34}S7$ of GCC (Table II).

The coordinates (r_s) of each substituted atom were calculated [50] according to the experimental rotational constants of parent and mono-substituted isotopologues determined for conformers TCC and GCC, respectively. The obtained results are listed in Table III. For conformer TCC, the MP2/6-311++G(d,p) calculated values of the coordinates (equilibrium structure, r_e) match

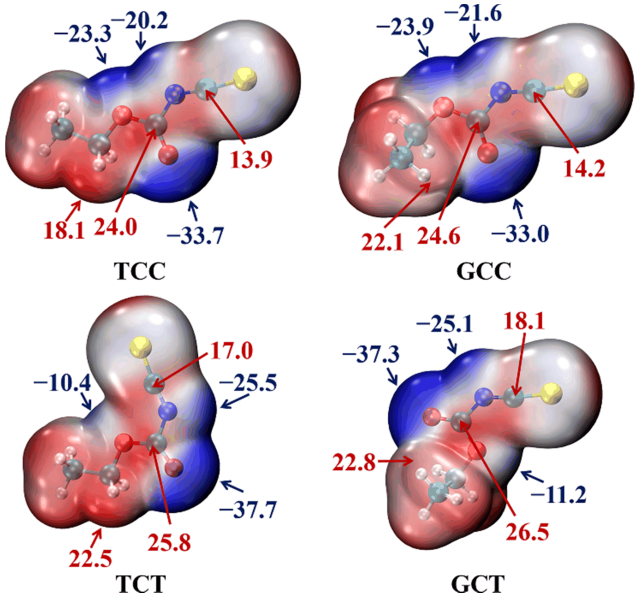

FIG. 3 Molecular electrostatic surface potentials (s=0.001 a.u.) of TCC, GCC, TCT, and GCT conformers calculated at the MP2/6-311++G(d,p) level of theory. The values of the most positive and most negative electrostatic potentials are given in kcal/mol.

the r_s values well, with the maximum deviation found for the N5 atom. This is likely due to the fact that N atom locates close to the center mass of TCC (see FIG. S2 in SM) and Kraitchman's method generates a relative inaccuracy estimation of the position of N atom. The P_{cc} value of the parent species of conformer TCC is determined to be 3.33 uÅ^2 (Table I), slightly larger than the P_{cc} value determined for the *trans* form of ethyl formate (3.23 uÅ^2) [51, 52] arising from the NCS substitution. The isotopic substitution of $^{13}C1$, $^{13}C2$, $^{13}C4$, $^{15}N5$, $^{34}S7$ do not change the P_{cc} value of TCC, indicating that these atoms are effectively located in the *ab*-plane and therefore a C_s symmetry is considered in the structural calculations for TCC. In addition, a structural fit [53] was performed to generate a partial effective structure (r_0) for TCC. Four bond lengths were fitted to reduce the difference between values of experimental and theoretical rotational constants while all other structural parameters were fixed to the r_e values (calculated at the MP2/6-311++G(d,p) level). The obtained atomic coordinates are also given in Table III. The corresponding r_s and r_0 structural parameters were calculated and compared with their r_e values in Table IV. For conformer GCC, the obtained r_s of coordinates of S7 agree with the r_e values well (Table III).

DOI:10.1063/1674-0068/cjcp2109177

TABLE III The r_s, r_0 and r_e coordinates of the conformers TCC and GCC.

Conformer	Atom	a/Å			b/Å		
		r_e[a]	r_s	r_0	r_e	r_s	r_0
TCC[b]	C1	−3.951	±3.9420(6)[c]	−3.95(1)	−0.720	±0.725(3)	−0.718(3)
	C2	−2.835	±2.8311(4)	−2.826(6)	0.301	±0.292(4)	0.304(6)
	C4	−0.500	±0.466(3)	−0.492(6)	0.331	±0.325(4)	0.328(1)
	C6	1.833	±1.8195(9)	1.83(2)	−0.285	±0.284(6)	−0.284(2)
	N5	0.630	±0.480(7)	0.623(9)	−0.506	±0.31(1)	−0.501(4)
	S7	3.386	±3.37414(1)	3.375(5)	−0.156	±0.15658(1)	−0.158(4)
GCC	S7[d]	−3.311	±3.3038(5)	−3.312(2)	0.093	±0.13(1)	0.090(3)

[a] Calculated at the MP2/6-311++G(d,p) level of theory.
[b] c-coordinates are fixed to zero due to symmetry.
[c] Values in the parentheses are 1σ errors given in units of the last digit.
[d] The r_e, r_s, and r_0 values of the c-coordinates of S7 are 0.154 Å, ±0.186(8) Å, 0.1604(7) Å, respectively.

TABLE IV The structural parameters (r_e, r_s and r_0) of conformer TCC.

Item	r_e	r_s	r_0
	Bond length/Å		
C2−C1	1.512	1.506(4)[a]	1.52(2)
N5−C4	1.406	1.138(9)	1.38(2)
C6−N5	1.223	1.340(7)	1.22(2)
S7−C6	1.559	1.560(1)	1.56(3)
	Bond angle/(°)		
∠C4C2C1	138.3	138.3(3)	[138.3][b]
∠C6N5C4	133.1	145.2(9)	[133.1][b]
∠S7C6N5	174.4	176.3(6)	[174.4][b]
	Dihedral angle/(°)		
∠S7C6N5C4	180	[180][b]	[180][b]

[a] Values in the parentheses are 1σ errors given in units of the last digit.
[b] Values fixed in the structural fit. Fixed at the r_e value due to symmetry.

IV. CONCLUSION

The conformational preference of ethoxycarbonyl isothiocyanate has been investigated using supersonic-jet FTMW spectroscopy and *ab inito* calculations. The first two most stable conformers of TCC and GCC have been detected in the supersonic jet. The observed rotational spectra of these two conformers show hyperfine splitting due to the quadrupole coupling effect of the ^{14}N nuclear. The two detected conformers are different in the relative orientation of the C1−C2−O3−C4 backbone with *trans* arrangement being more stable than that of *gauche* one. For the most stable conformer (TCC), the measurements of the ^{13}C, ^{15}N, and ^{34}S isotopologues lead to an accurate determination of its molecular structure. These accurate rotational spectroscopic parameters can be used to predict rotational transitions in higher frequencies or used directly for identifying transition lines from astronomical observations. Especially, ethyl formate ($CH_3CH_2OC(=O)H$), a molecule can be taken as the precursor of EIC, has been detected in Sagittarius B2(N) and Orion B [54, 55]. This identification suggests EIC to be a candidate for astronomical observations.

Supplementary materials: The 8 possible configurations for EIC monomer (FIG. S1), geometries and principal axes of inertia of TCC of EIC calculated at the MP2/6-311++G(d,p) level of theory (FIG. S2), the potential energy surfaces connecting the interconversion of TCC and GCC, TCC and TCT, and GCC and GCT calculated at the MP2/6-311++G(d,p) level of theory (FIG. S3), MP2/6-311++G(d,p) calculated spectroscopic parameters of ethoxycarbonyl isothiocyanate (Table S1), and measured transition lines for TCC and GCC (Tables S2−S10) are all available.

V. ACKNOWLEDGMENTS

The support from the National Natural Science Foundation of China (No.22273009) and Chongqing University is gratefully acknowledged.

[1] A. K. Mukerjee and R. Ashare, Chem. Rev. **91**, 1 (1991).

[2] M. Avalos, R. Babiano, P. Cintas, J. L. Jimenez, and J. C. Palacios, Heterocycles **33**, 973 (1992).
[3] B. A. Trofimov, J. Heterocycl. Chem. **36**, 1469 (1999).
[4] Y. S. Keum, W. S. Jeong, and A. T. Kong, Mutat. Res. Fundam. Mol. Mech. Mutagen. **555**, 191 (2004).
[5] P. Talalay and J. W. Fahey, J. Nutr. **131**, 3027S (2001).
[6] S. Kawakishi and T. Kaneko, Phytochemistry **24**, 715 (1985).
[7] S. Kawakishi and T. Kaneko, J. Agric. Food Chem. **35**, 85 (1987).
[8] P. J. Delaquis and P. L. Sholberg, J. Food Prot. **60**, 943 (1997).
[9] K. Isshiki, K. Tokuoka, R. Mori, and S. Chiba, Biosci. Biotechnol. Biochem. **56**, 1476 (1992).
[10] K. Kyung and H. Fleming, J. Food Prot. **60**, 67 (1997).
[11] C. M. Lin, J. Kim, W. X. Du, and C. I. Wei, J. Food Prot. **63**, 25 (2000).
[12] T. Ogawa and K. Isshiki, Nippon Shokuhin Kogyo GakkaiShi **43**, 535 (1996).
[13] B. Shofran, S. Purrington, F. Breidt, and H. Fleming, J. Food Sci. **63**, 621 (1998).
[14] S. M. Ward, P. J. Delaquis, R. A. Holley, and G. Mazza, Food Res. Int. **31**, 19 (1998).
[15] W. Kasten and H. Dreizler, Zeitschrift für Naturforschung A **42**, 79 (1987).
[16] J. R. Durig, X. Zhou, A. M. El Defrawy, G. A. Guirgis, T. K. Gounev, and C. Zheng, J. Mol. Struct. **839**, 107 (2007).
[17] Y. Xu, J. Zhang, W. Li, J. Li, and G. Feng, ACS Earth Space Chem. **5**, 33 (2021).
[18] R. Glaser, R. Hillebrand, W. Wycoff, C. Camasta, and K. S. Gates, J. Org. Chem. **80**, 4360 (2015).
[19] W. Sun, R. L. Davis, S. Thorwirth, M. E. Harding, and J. van Wijngaarden, J. Chem. Phys. **149**, 104304 (2018).
[20] J. Stitsky, W. G. Silva, W. Sun, and J. van Wijngaarden, J. Phys. Chem. A **124**, 3876 (2020).
[21] M. Ge, C. Ma, S. Tong, W. Xue, Z. Pu, and D. Wang, New J. Chem. **33**, 2155 (2009).
[22] L. A. Ramos, S. E. Ulic, R. M. Romano, M. F. Erben, C. W. Lehmann, E. Bernhardt, H. Beckers, H. Willner, and C. O. Della Védova, Inorg. Chem. **49**, 11142 (2010).
[23] L. A. Ramos, S. E. Ulic, R. M. Romano, Y. V. Vishnevskiy, N. W. Mitzel, H. Beckers, H. Willner, S. Tong, M. Ge, and C. O. D. Védova, J. Phys. Chem. A **117**, 5597 (2013).
[24] L. A. Ramos, S. E. Ulic, R. M. Romano, H. Beckers, H. Willner, and C. O. D. Védova, J. Phys. Chem. A **118**, 697 (2014).
[25] R. Feng, Z. Wu, and X. Zeng, J. Mol. Struct. **1172**, 25 (2018).
[26] A. T. Bech, R. Flammang, C. T. Pedersen, M. W. Wong, and C. Wentrup, J. Chem. Soc. Perkin Trans. **2**, 1869 (1999).
[27] W. Sun, W. G. Silva, and J. van Wijngaarden, J. Phys. Chem. A **123**, 2351 (2019).
[28] T. Balle and W. Flygare, Rev. Sci. Instrum. **52**, 33 (1981).
[29] J.-U. Grabow, W. Stahl, and H. Dreizler, Rev. Sci. Instrum. **67**, 4072 (1996).
[30] G. G. Brown, B. C. Dian, K. O. Douglass, S. M. Geyer, S. T. Shipman, and B. H. Pate, Rev. Sci. Instrum. **79**, 053103 (2008).
[31] J.-U. Grabow, *Fourier Transform Microwave Spectroscopy Measurement and Instrumentation*, in *Handbook of High-Resolution Spectroscopy*, M. Quack and F. Merk Eds., Chicester: John Wiley & Sons, Ltd., 723−799 (2011).
[32] M. Frerking, R. Linke, and P. Thaddeus, Astrophys. J. **234**, L143 (1979).
[33] D. Halfen, L. Ziurys, S. Brünken, C. Gottlieb, M. McCarthy, and P. Thaddeus, Astrophys. J. Lett. **702**, L124 (2009).
[34] J. Cernicharo, C. Cabezas, M. Agúndez, B. Tercero, J. Pardo, N. Marcelino, J. Gallego, F. Tercero, J. López-Pérez, and P. de Vicente, Astron. Astrophys. **648**, L3 (2021).
[35] B. A. McGuire, Astrophys. J. Suppl. Ser. **239**, 17 (2018).
[36] J. Durig, J. Sullivan, T. Little, and S. Cradock, J. Mol. Struct. **118**, 103 (1984).
[37] S. Maiti, A. Jaman, and R. Nandi, J. Mol. Spectrosc. **165**, 168 (1994).
[38] W. Caminati, J. Mol. Struct. **190**, 227 (1988).
[39] M. A. King, H. W. Kroto, and B. Landsberg, J. Mol. Spectrosc. **113**, 1 (1985).
[40] B. P. Winnewisser, M. Winnewisser, I. R. Medvedev, M. Behnke, F. C. De Lucia, S. C. Ross, and J. Koput, Phys. Rev. Lett. **95**, 243002 (2005).
[41] W. Sun, W. G. D. P. Silva, and J. van Wijngaarden, J. Phys. Chem. A **123**, 2351 (2019).
[42] J. Koput, J. Mol. Spectrosc. **118**, 189 (1986).
[43] J.-U. Grabow, Q. Gou, and G. Feng, *72nd International Symposium on Molecular Spectroscopy*, Champaign-Urbana, (2017).
[44] M. J. Frisch, G. W. Trucks, H. B. Schlegel, G. E. Scuseria, M. A. Robb, J. R. Cheeseman, G. Scalmani, V. Barone, G. A. Petersson, H. Nakatsuji, X. Li, M. Caricato, A. V. Marenich, J. Bloino, B.G. Janesko, R. Gomperts, B. Mennucci, H. P. Hratchian, J. V. Ortiz, A. F. Izmaylov, J. L. Sonnenberg, D. Williams-Young, F. Ding, F. Lipparini, F. Egidi, J. Goings, B. Peng, A. Petrone, T. Henderson, D. Ranasinghe, V. G. Zakrzewski, N. R. J. Gao, G. Zheng, W. Liang, M. Hada, M. Ehara, K. Toyota, R. Fukuda, J. Hasegawa, M. Ishida, T. Nakajima, Y. Honda, O. Kitao, H. Nakai,

DOI:10.1063/1674-0068/cjcp2109177

T. Vreven, K. Throssell, J. A. Montgomery Jr., J. E. Peralta, F. Ogliaro, M. J. Bearpark, J. J. Heyd, E. N. Brothers, K. N. Kudin, V.N. Staroverov, T. A. Keith, R. Kobayashi, J. Normand, K. Raghavachari, A. P. Rendell, J. C. Burant, S. S. Iyengar, J. Tomasi, M. Cossi, J. M. Millam, M. Klene, C. Adamo, R. Cammi, J. W. Ochterski, R. L. Martin, K. Morokuma, O. Farkas, J. B. Foresman, and D. J. Fox, *Gaussian 16, Revision A.03*, Wallingford, CT: Gaussian Inc., (2016).

[45] M. J. Frisch, M. Head-Gordon, and J. A. Pople, Chem. Phys. Lett. **166**, 275 (1990).

[46] R. Krishnan, J. S. Binkley, R. Seeger, and J. A. Pople, J. Chem. Phys. **72**, 650 (1980).

[47] J. K. Watson, *Vibrational Spectra and Structure*, Amsterdam: Elsevier, (1977).

[48] H. M. Pickett, J. Mol. Spectrosc. **148**, 371 (1991).

[49] R. Ruoff, T. Klots, T. Emilsson, and H. Gutowsky, J. Chem. Phys. **93**, 3142 (1990).

[50] J. Kraitchman, Am. J. Phys. **21**, 17 (1953).

[51] J. M. Riveros, and E. B. Wilson Jr., J. Chem. Phys. **46**, 4605 (1967).

[52] I. R. Medvedev, F. C. De Lucia, and E. Herbst, Astrophys. J. Suppl. Ser. **181**, 433 (2009).

[53] Z. Kisiel, J. Mol. Spectrosc. **218**, 58 (2003).

[54] A. Belloche, R. Garrod, H. Müller, K. Menten, C. Comito, and P. Schilke, Astron. Astrophys. **499**, 215 (2009).

[55] B. Tercero, I. Kleiner, J. Cernicharo, H. Nguyen, A. López, and G. M. Caro, Astrophys. J. Lett. **770**, L13 (2013).

DOI:10.1063/1674-0068/cjcp2109177